Impact of PWM strategies on RMS current of the DC-link Voltage Capacitor of a dual-three phase drive

ROUHANA Najib
DUGUEY Jean-François
VALEO-VEM
2 rue André BOULLE
94046 CRETEIL Cedex – FRANCE
rouhana.najib@gmail.com

SEMAIL Eric
L2EP
ARTS et METIERS
8 Bd Louis XIV
LILLE-FRANCE
eric.semail@ensam.eu

***Abstract*—The major drawback of usual dual three-phase AC machines, when supplied by a Voltage Source Inverter (VSI), is the occurrence of extra harmonic currents which circulate in the stator windings causing additional losses and constraints on the power component. This paper compares dedicated Pulse Width Modulation (PWM) strategies used for controlling a dual three-phase Permanent Magnet Synchronous machine supplied by a six-leg VSI. Since the application is intended for low-voltage (48V) mild-hybrid automotive traction, an additional major constraint arises: the compactness of the drive related to the size of the DC-bus capacitor. Thus, the PWM strategy must be chosen by taking into consideration its impact on both, the motor and the RMS value of DC-bus current.**

Keywords: Dual three-phase synchronous machine, multiphase drive, six-phase voltage source inverter, PWM.

I. INTRODUCTION

Commonly supplied in the past by Current Source Inverter with thyristors for fault-tolerant applications such as marine propulsion, dual-three phase AC machines, are now also supplied by Voltage Source Inverters, thus allowing the use of induction or PM synchronous machines. In comparison with three-phase drives, these machines also show less pulsating torques even with the presence of five and seven harmonics of electromotive force (emf) since the first harmonic of current does not interact with these two harmonics of emf [1]. As a consequence they are attractive for automotive application such as steering-by-wire [2] since fault tolerance and low torque pulsations, even with non-sinusoidal emf, are then desired.

The main problem of these machines is the presence of parasitic currents which can appear in stator phase if the control of the Voltage Source Inverter is not appropriate. Oversizing of power component can be then necessary. This problem has been addressed in several papers: in [3] coupled filter and synchronization between the six legs of the VSI were already proposed; in [4], the importance of considering the second characteristic subspace of a dual-three phase AC machine was pointed out in order to explain why parasitic currents of high amplitude can appear. This subspace which is associated with the five and seven harmonics [1] is characterized by an inductance whose value is equal to the leakage inductance in case of sinusoidal magneto-motive force. So, the PWM can induce important parasitic currents if the switching frequency is not sufficiently high.

Papers have then studied different strategies of PWM in order to minimize these parasitic currents either with SVM or with more classical carrier based ones [5][6][7][8][9].

More recently, predictive control has also been proposed to improve the performances [10] for induction machines. For synchronous machine, [11] points out as in [1] the particularity of the impact of harmonics of emf on the constraints for the control: if the PWM strategy imposes always a null zero-sequence average voltage in the second characteristic subspace of the machine fifth and seven harmonics of current can be induced by the fifth and seven harmonics of emf.

The specificity of the proposed paper is to consider another parameter for the choice of the strategy of PWM: the sizing of the DC-link capacitor. This point is particularly important with low voltage (< 48V) and significant power (> 10kW) such as used in automotive applications, the problem is particularly sensitive since it is necessary to use several capacitors in parallel in order to obtain the global adequate value.

It is possible to judge from Figure 1 on the importance of the relative volume of the DC-bus capacitor in comparison with the whole converter. A minimization of the RMS current in the DC-bus will not only reduce the losses in the capacitor but also will have an impact on the volume of the capacitor by restricting the constraints.

Moreover, the weak value of the DC-link voltage makes it sensitive to each voltage drop such as in power component and connections, but also in capacitors, with a potential impact on the stability of the voltage DC-link.

For three phase high density drives, this impact has been studied with specific PWM strategies either to reduce the RMS current [12][13][14] or to stabilize the voltage [15].

For multiphase machines it has been shown that for square-wave supplies [16] the increase of the phase number allows to decrease the RMS value of the DC current. More precisely for dual-three phase induction machine, [17] has studied the impact, on the RMS DC-current, of classical carrier-based PWM with and without third harmonic injection.

In the proposed paper a PWM strategy which minimizes the DC-link RMS current will be compared with other strategies which classically optimizes the currents of the dual-three phase machine.

This paper is organized as follows.

Section II provides an equivalent multi-machine multi-inverter model in order to segregate the control parameters of the inverter.

Section III focuses on defining the distribution of tasks between the three independent fictitious inverters which models, in average approach, the real inverter.

Section IV provides comparison results of PWM strategies.

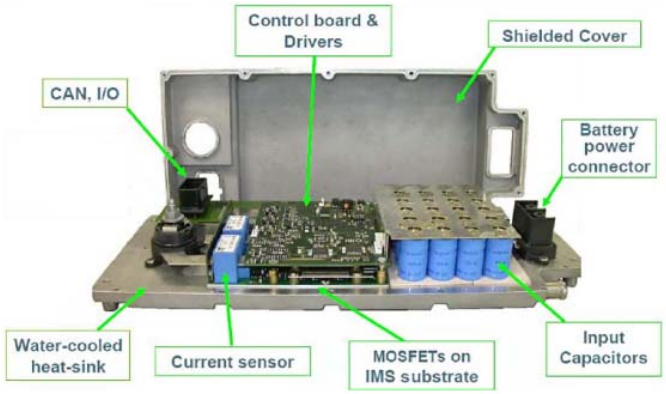

Figure 1: Exhibition of high volume of DC-capacitor in a mild-hybrid low-voltage automotive application [12]

II. Modeling of the Six-Phase Drive

A. Multi-Machine modeling of the Six-Phase Machine

In order to obtain a synthetic modelling of the global drive and to deduce by systematic rules the organization of the control in its structure and strategies, we use a graphical formalism (see detail in appendix) focused on energy flows representation called Energetic Macroscopic Representation (EMR)[18]. This tool is associated with the multi-machine theory [1] which splits a multiphase machine in a few two-phase dq-type machines. In Figure 2 is represented a dual-three phase machine which can be considered equivalent to three two-phase machines (M1, M2, and M3) [1] where machine M3 is never supplied as a double-star connection is adopted. With the assumption of a machine with sinusoidal emf, only the emfs and currents of machine M1 will produce the torque with the consequence that four degrees of freedom are available for the control of the parasitic AC currents and RMS DC current. If fifth and/or seventh harmonic of emf exist then it will remain only two degrees of freedom since the torque of the M2 machine have to be controlled.

B. Multi-VSI Modeling of the Six-leg VSI

As long as the working conditions are in the linear domain with no saturation of the inverter, it can then be considered that a six-leg Voltage Source Inverter (VSI) is equivalent to three VSIs, each one being able to impose an independent average voltage in a plane which is associated with one of the three fictitious machines described in paragraph A.

Thus, it is possible to represent the VSI with Energetic Macroscopic Representation as in Figure 3, in accordance with the energetic representation of the dual-three phase machine.

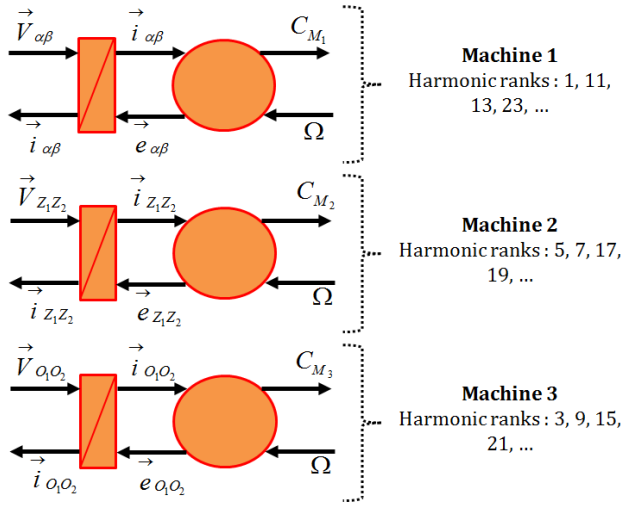

Figure 2: Energetic Macroscopic Representation of the three fictitious machines equivalent to a double-three phase machine after Concordia transformation

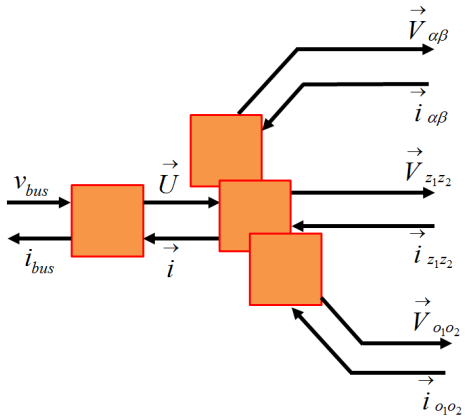

Figure 3: Energetic Macroscopic Representation of the Voltage Source Inverter

The voltage vectors produced by the inverter in the natural basis will be analyzed from a different perspective. To do so, the Concordia transformation will be applied by projecting the 2^6=64 natural basis vectors to the fictitious machines M1, M2 and M3 frames. Thus, three new bi-dimensional bases are defined. In Figure 4 are represented the two VSIs that will be used for the control of the machine. For each machine (M1 and M2) the average vector will be generated by a controller in order to impose the desired currents. In case of sinusoidal electromotive force, only sinusoidal currents must be imposed in M1 machine by the control of the VSI1 and the average voltage imposed by the VSI2 must be equal to zero. With non-sinusoidal emf, the current feedback in machine M2 will impose the adequate average voltage vector reference that will be supplied by the VSI2. Concerning inverter voltage vectors of the zero-sequence machine M3, choice can be done for optimization since it is the double-neutral winding connection which ensures zero-sequence currents. The resultant system is a four dimensional system, and the control of the dual-three phase machine is further simplified.

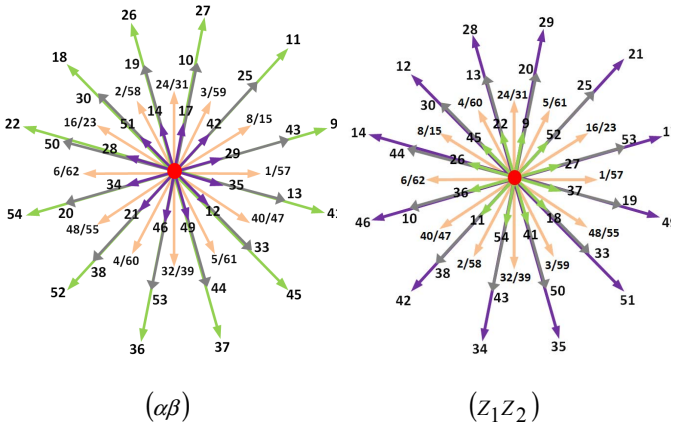

Figure 4: 64 space voltage vectors of six-phase VSI in the planes (αβ) and (Z_1Z_2)

The representation of the global system is shown in Figure 5. The generalized Concordia transformation is represented with an electrical coupling.

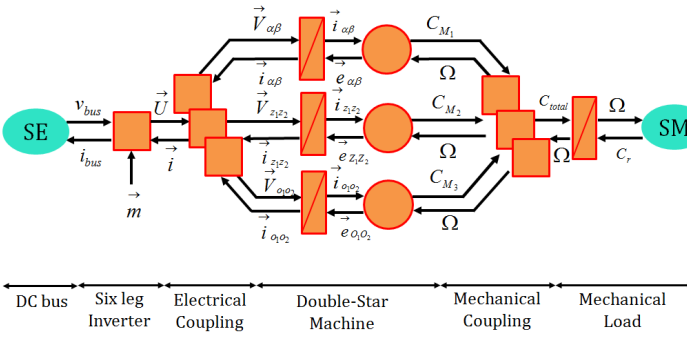

Figure 5: Modeling of the global system

The energy distribution operated with the Concordia transformation also naturally respects the harmonics distribution depicted in Figure 2. Concretely, this means that machine M1 is only supplied with voltage harmonics of ranks 1, 11, 13, 23, … while machine M2 is supplied with voltage harmonics of ranks 5, 7, 17, 19 … Concerning the zero-sequence M3 machine, it is supplied with voltage harmonics of ranks 3, 9, 15, 21 … No interaction exists between these harmonic families and every fictitious machine creates its own torque. The total torque C_{total} is the sum of C_{M1}, C_{M2} and C_{M3}. This approach will contribute in organizing the control structure by an inversion of the energy chain. For conversion blocks, the inversion can be directly established as to energy accumulation blocks, the inversion needs a controller with its associated measurements (Figure 7). Thus, controllers are used to control the currents of the three fictitious machines. The representation of Figure 6 fits with the control of the torque reference which is split into three components C_{M1ref}, C_{M2ref} and C_{M3ref}. Then, these references are transformed into current references, inversing the electromechanical conversion blocks. The currents are controlled using PI controllers (with a disturbance compensation), leading to the voltage references. At last, the inverse Concordia transformation leads to the voltage reference expressed in the natural UVWXYZ frame.

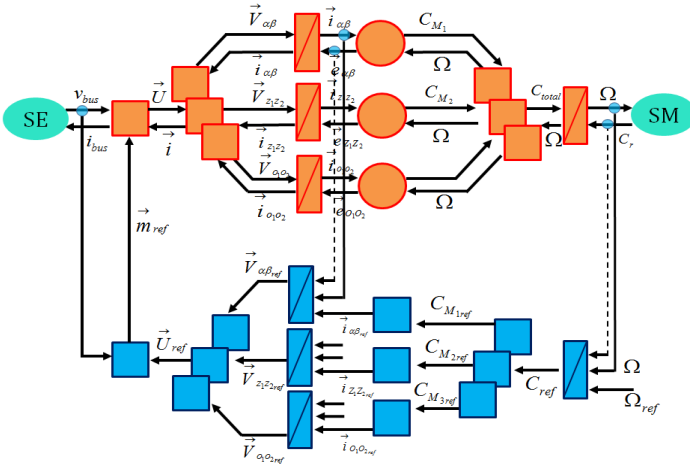

Figure 6: Inversion based control structure

We should note that M1 currents can be controlled in a rotating Park frame, exactly as it is generally done for standard three-phase drives.

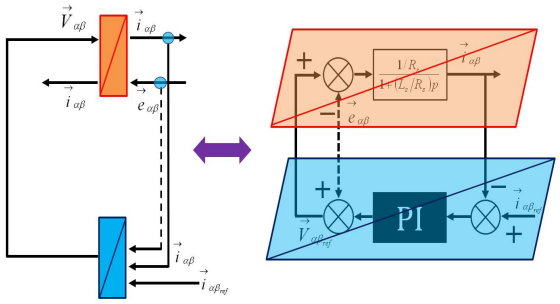

Figure 7: Energy accumulation blocks with its appropriate inversion based control structure

III. Space Vector Control for Choice of PWM

Practically, it is known that pulsating torques, associated with low frequency harmonic of currents, and high frequency parasitic currents depend on the choice of the PWM strategy.

Even if null average currents $\vec{i}_{z_1z_2}$ are imposed in the M2 machine thanks to null average voltage in VSI2, the practical performances in terms of quality will depend on what happens in this M2 machine more than in the main M1 machine at the origin of the average torque. The analysis of the voltage vectors which are activated in the VSI2 are then of great importance.

For the last two components of fictitious voltages imposed by the VSI 3, the impact is null on the machine since the two star connections ensure the nullity of the currents in the M3 machine, whatever the stress imposed by the VSI 3. Only common-mode currents can be induced by the choice of the vectors of VSI3.

A. PWM constraints for the control of the average torque

In the *(αβ)* plane of the machine M1, characterized by a sinusoidal electromotive force $e_{\alpha\beta}$, the average voltage reference vector $V^*_{\alpha\beta}$ describes thus a circular trajectory (see Figure 9). For that, minimizing pulsating torques requires

choosing the voltage command vectors as close as possible to the circle described by the average voltage reference vector.

B. *PWM constraints for minimization of Copper Losses and torque pulsations in the motor*

While taking in consideration that the average currents in the second fictitious machine M2 do not produce average torque, it is interesting to be able to eliminate them in order to minimize losses. Taking into account the fact that emf are null or weak in the (Z_1Z_2) plane, a PWM strategy which uses low amplitude voltage vectors in the (Z_1Z_2) plane appears as a good means to minimize easily the amplitude of parasitic current induced by the modulation.

C. *PWM constraints for minimization of RMS current in the DC-bus Capacitor*

In sections II.A and II.B, the constraints concern mainly average current and voltages of the VSI1 and VSI2. The third inverter has no impact on the electrical machine. Thus, it can be used to achieve an over modulation by injecting a third harmonic voltage in order to better exploit the DC bus voltage. As long as this over modulation is not necessary, we can also propose using it in order to minimize the RMS value of the DC capacitor current.

Concerning the latter one, it is rather the high frequency components of the current which are important. Thus, it is interesting to define a global PWM for the global minimization of the DC link's RMS current. The time sequence of the chosen vectors for obtaining the average values is of the utmost importance.

IV. COMPARISON OF PWM FOR RMS DC-CURRENT

A. *PWM for RMS DC-current-minimization*

The scheme of a six phase voltage source inverter which is used in this investigation is shown in Figure 8. Each phase of the load is represented by a series connection of an emf, a resistance and an inductance. The DC side is represented by a series connection of a ripple-free constant DC voltage source.

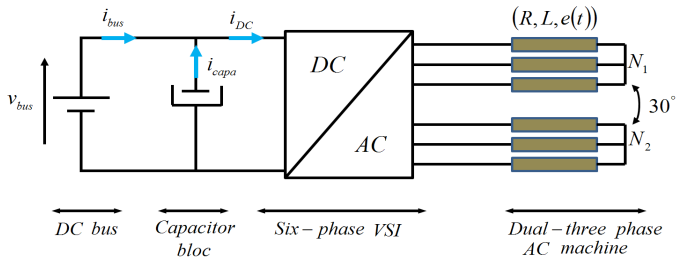

Figure 8 : Six-leg Voltage Source Inverter

A capacitor is connected in parallel with the input of the inverter to absorb the ripple current which is generated by the inverter and to reduce the voltage fluctuation across the input terminal of the inverter.

The DC capacitor current is dependent of three parameters:

- The rotor's position angle : θ ;
- The phase shift angle between the fundamental of the output voltage vector and current vector : φ
- The modulation factor : $m = \frac{\hat{V}}{v_{bus}/2}$

The modulation factor is a controlled variable imposed by the reference input while the phase shift angle between the fundamental's output voltage vector and the current vector is a variable imposed by the dual three-phase machine.

The question is, among the 64 possibilities, which command voltage vectors are to be used in order to minimize the RMS value of the capacitor current? Since the determination of the analytical expression of the DC bus current is not obvious in our case of application, an OFF-line calculus script, using MATLAB platform, was developed. For each command sequence, the effect of each instantaneous voltage vector on the evolution of the RMS DC bus ripple current absorbed by the capacitor, defined by (1), is tested.

$$i_{Capa}^{RMS} = \sqrt{\left(i_{DC}^{RMS}\right)^2 - \left\langle i_{DC}\right\rangle^2} \qquad (1)$$

We should note that the RMS capacitor current is the standard deviation of the inverter instantaneous input current i_{DC}. The latter is the sum of the contributions from all the inverter legs and is expressed as follows:

$$i_{DC} = \vec{S}.\vec{i} = \sum_{k=1}^{6} S_k\, i_k \qquad (2)$$

Where $\vec{S}$ and $\vec{i}$ are the inverter switching vector ($S_k \in \{0,1\}$) and the load current vector respectively. The sequence of vectors which, for each modulation factor and every phase shift angle, reduces the criteria defined by equation (1) is to be selected. So, for each functioning point, we have a specific set of command voltage vectors.

B. *Results with different PWM strategies*

1) *With strategies C6_SVPWM, DZSI, SVPWM focused on machine currents*

As it is mentioned in section III.B, conventional PWM strategies are focused on the quality of the currents of the machine. We have chosen for the comparison the C6_SVPWM strategy described in [7], the DZSI (Double Zero-Sequence Sequence Injection) strategy described in [19] and also the classical SVPWM in [20] for three-phase machines. The DZSI strategy is the extension to the six-phase case of the common three-phase SVPWM zero-sequence injection technique.

For C6_SVPWM, as it is appearing in Figure 9 four adjacent voltage vectors are always selected from the vectors which span the outermost polygon on the $(\alpha\beta)$ plane according

to the position of the reference voltage vector $V^*_{\alpha\beta}$. The fifth vector is chosen from the zero vectors located at the *(αβ)* plane origin. For example, as indicated by the dots in Figure 9, voltage vectors *41*, *9*, *11,* and *27* are selected when the reference voltage vector lies inside the triangle area between voltage vectors *9* and *11*. The four voltage vectors spread out to cover the *(Z_1Z_2)* plane, thus making it possible for the average voltage in this plane be zeroed during every sampling interval.

It is also noted that the chosen vectors in the *(Z_1Z_2)* plane have the smallest amplitude. Therefore, the proposed space vector PWM strategy will offer the maximum voltage output capability on the *(αβ)* plane while keeping the harmonics on the *(Z_1Z_2)* plane at a minimum.

The proposed control technique has been simulated and the results, for a single operating point at nominal conditions (*m=1, φ=0°*, with a nominal mechanical speed of 3000 rpm), are shown in Figure 10.

Since the modulation factor *m* is imposed by the reference input and the phase shift angle *φ* is imposed by the machine, the role of inverter is to adapt to the variation of *φ* while controlling the modulation factor. The calculus script developed using MATLAB platform (which aims to reduce the RMS DC bus ripple current absorbed by the capacitor block) has delivered optimal results, each corresponding to a sequence of voltage vectors to be used for each operating point (*m*, *φ*). Figure 10 shows the results for *m=1* and $\varphi \in [0°,90°]$. It can be seen that, in contrary with previous strategies, the activated vectors and the associated sequence used by 6_DC_RMS_PWM strategy are dependent on the operating point. Figure 11 and Figure 12 compare, for various PWM strategies, the DC bus capacitor RMS current and the machine current ripple for *m=0.7* and $\varphi \in [0°,90°]$. As it can be seen, an optimal result in terms of RMS DC bus ripple current does not match the conventional PWM strategies. The proposed 6_DC_RMS_PWM shows, of course, the best result in terms of RMS DC-link current in comparison with other PWM strategies which are better for the machine current ripples. On the contrary, this strategy induces large amplitudes of undesired harmonic machine currents (even without harmonics of emf). It can be considered that it is due to the non-linear behavior of the VSI which is induced by frequent change of voltage vector as remarked in Figure 10. Adding to that, a simple examination of the sequences presented, shows that for each switching period, each bridge changes its state more than twice thus the switching frequency may not be maintained at the same level.

Results from Figure 11 show also that the conventional DZSI and the C6_SVPWM provide close results in terms of PWM current ripples. On the other hand, both strategies have different impact on the DC bus side for high values of *φ* angle: the conventional DZSI strategy appears as more performant than the C6_SVPWM.

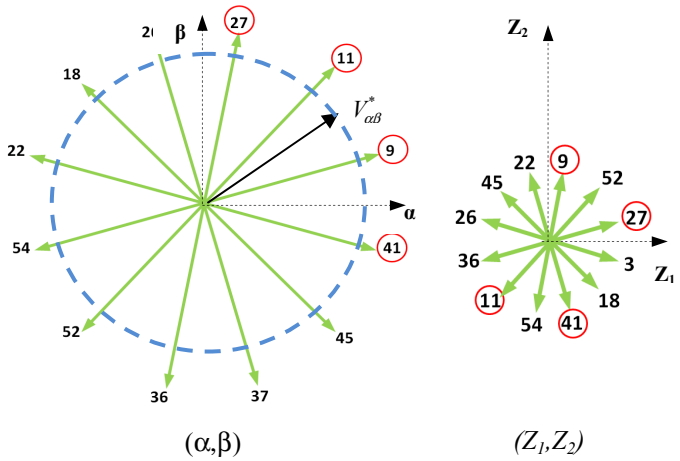

Figure 9: Inverter voltage vectors corresponding to the chosen switching modes for C6_SVPWM strategy

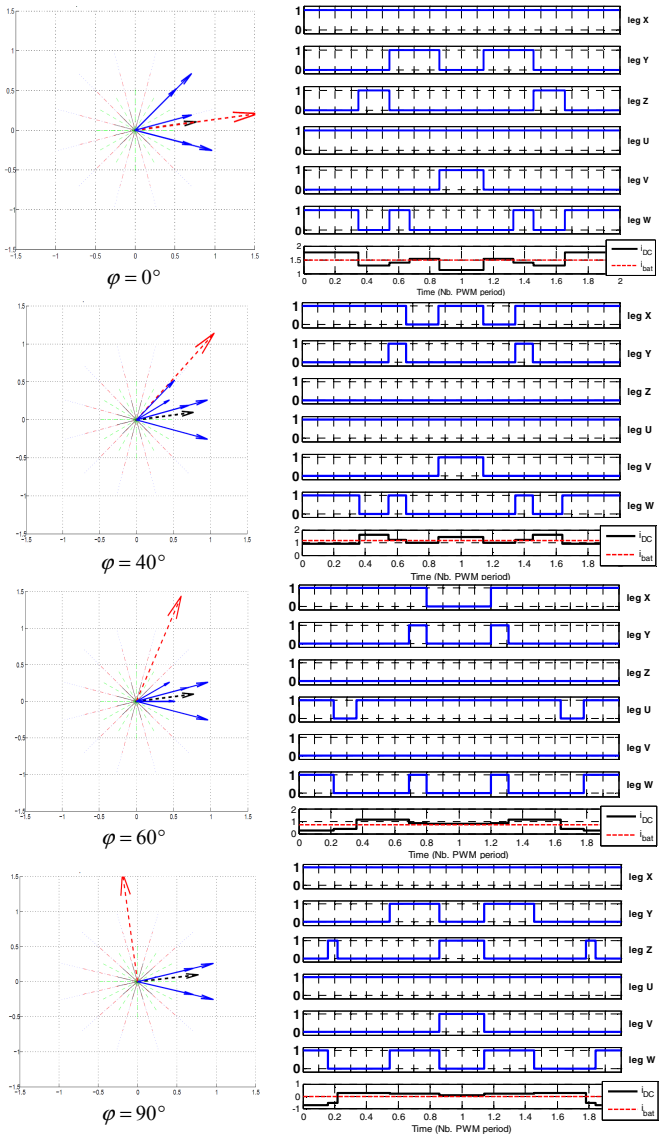

Figure 10: Switching modes selection for each operating point (m=1,φ) of 6_DC_RMS_PWM– The black arrow: V_αβ, the red arrow : I_αβ and the blue arrows : voltage command vectors

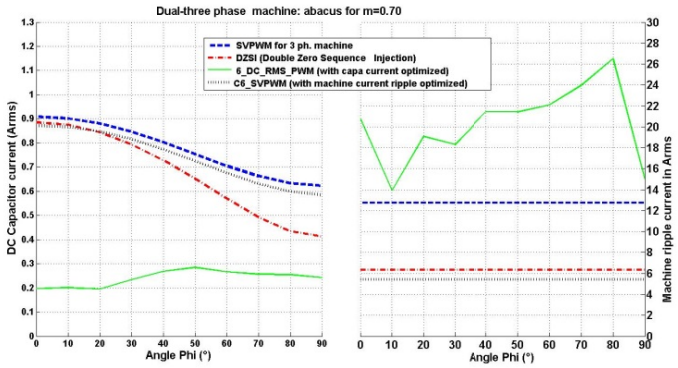

Figure 11: Comparison between 3 Classical PWM and 6_DC_RMS_PWM: Effect on the DC link side (left) and on the machine side (right)

V. Conclusion

In this paper, a PWM strategy (6_DC_RMS_PWM) dedicated to the minimization of the DC bus RMS current is compared with more conventional ones whose objectives are rather the quality of the machine current. Simulation results show that significant differences appear for the level of the RMS of DC current between the 6_DC_RMS_PWM and the other ones. The DZSI appears as the best of the conventional PWM for the DC current. It appears also that the quality of the machine current is low with the 6_DC_RMS_PWM. There are moreover large fluctuations due to the changes of sectors used for the minimization of the RMS DC current. So, in order to minimize the size of the DC capacitor it is necessary to define PWM strategies which take into account both constraints simultaneously.

VI. Appendix

EMR is a graphical description, which organizes the system into interconnected basic elements [EMR website]: sources of energy (green ovals), accumulations of energy (orange crossed rectangles), mono-physical (orange squares) or multi-physical conversions (orange circles), and coupling elements (distributions of energy, double orange squares or circles) (see TABLE I). All elements are connected according to the action and reaction principle [21]. The product of the action and reaction variables between two elements leads to the instantaneous power exchanged. Furthermore, all the components are described respecting the physical causality: i.e. the integral causality.

An inversion-based control structure can be systematically deduced from the EMR using inversion rules [22]. Conversion elements are directly inverted (blue parallelograms) and accumulation elements are inverted using closed-loop controllers (crossed blue parallelograms). Moreover, inversions of coupling elements require distribution coefficients (double blue parallelograms), which allocate the

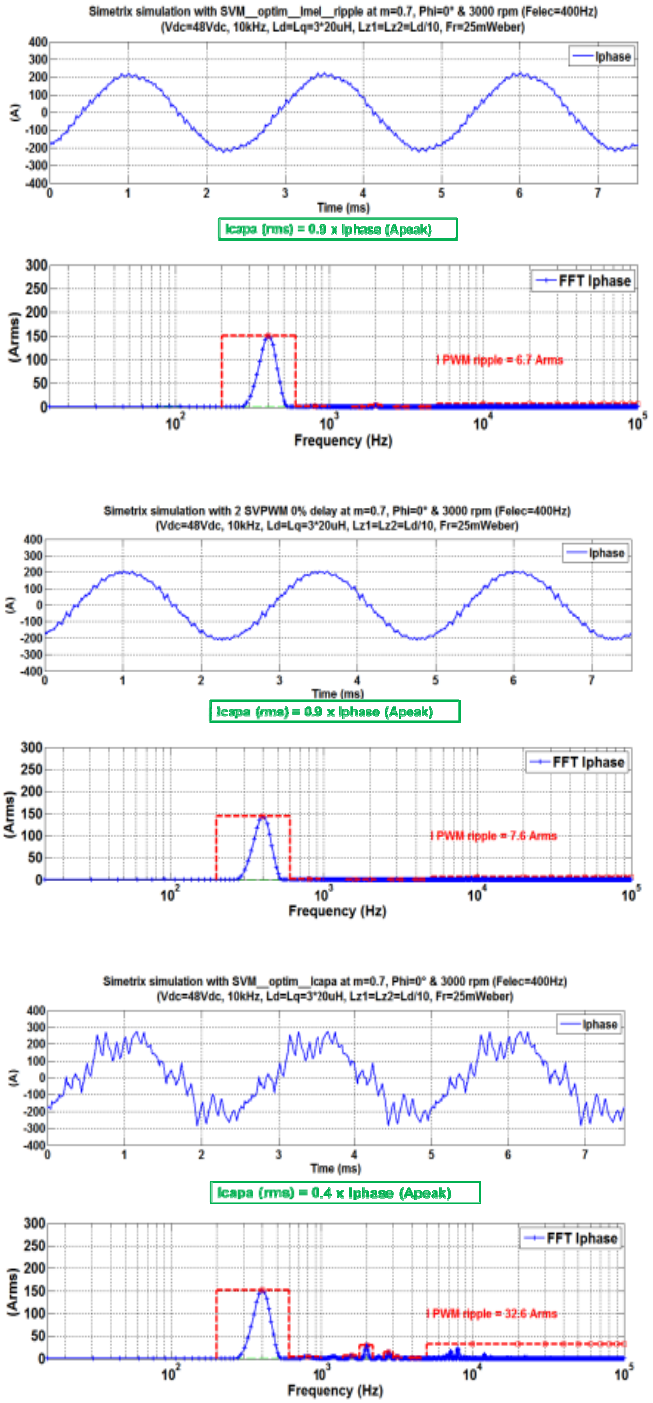

Figure 12:

For three PWM strategies (from high to low :C6_SVPWM, DZSI and 6_DC_RMS_PWM), time waveforms for one-phase stator current component and total harmonic distortion for the same phase stator current component. (m=0,7, φ=0°, 3000 rpm)

distribution of energy within the system.

TABLE I ;EMR PICTOGRAMMS

[EMR. Website]: http://www.emrwebsite.org/, consulted in 2014.

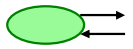	Energy sources	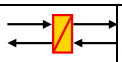	Energy accumulation element	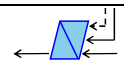	Closed loop control
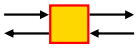	Mono-physical conversion element	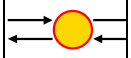	Multi-physical conversion element		Open loop control (direct inversion)
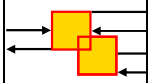	Mono-physical coupling (energy distribution)	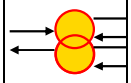	Multi-physical coupling (energy distribution)	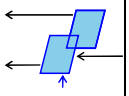	Coupling inversion with criteria
	Action – Reaction variables		Sensor		Strategy level

VII. REFERENCES

[1] E. Semail, A. Bouscayrol and J. P. Hautier, "Vectorial formalism for analysis and design of polyphase synchronous machines," EPJ AP (European Physical Journal-Applied Physics), vol. 22 no 3, June 2003, pp. 207-220.

[2] N. Bianchi, S. Bolognani, M. D. Pre, M. Tomasini, L. Peretti, M. Zigliotto, "The steering effect PM motor drives for automotive systems," IEEE Ind. Appl. Mag., vol. 14, no. 2, pp. 40–48, Mar./Apr. 2008.

[3] G. Gierse and W. Schuermann, "Microprocessor control for two magnetically coupled three-phase PWM inverters," IEEE Trans. Power Electron., vol. PE-1, no. 3, pp. 141–147, Jul. 1986.

[4] Y. Zhao and T. A. Lipo, "Space vector PWM control of dual three phase induction machine using vector space decomposition," IEEE Trans. Ind.Appl., vol. 31, no. 5, pp. 1100–1109, Sep./Oct. 1995.

[5] R. Bojoi, A. Tenconi, F. Profumo, G. Griva, and D. Martinello, "Complete analysis and comparative study of digital modulation techniques for dual three-phase AC motor drives," Proc. on PESC, Cairns, Australia, 2002, pp. 851–857.

[6] R. Bojoi, M. Lazzari, F. Profumo, and A. Tenconi, "Digital field-oriented control for dual three-phase induction motor drives," IEEE Trans. Ind. Appl., vol. 39, no. 3, pp. 752–760, May/Jun. 2003.

[7] D. Hadiouche, L. Baghli, and A. Rezzoug, "Space-vector PWM techniques for dual three-phase AC machine: Analysis, performance evaluation, and DSP implementation," IEEE Trans. Ind. Appl., vol. 42, no. 4, pp. 1112–1122, Jul./Aug. 2006.

[8] K. Marouani, L. Baghli, D. Hadiouche, A. Kheloui, and A. Rezzoug, "A new PWM strategy based on a 24-sector vector space decomposition for a six-phase VSI-fed dual stator induction motor", IEEE Trans. Ind. Electron., vol. 55, no. 5, pp. 1910–1920, May 2008.

[9] D. Yazdani, S. Khajehoddin, A. Bakhshai, and G. Joós, "Full utilization of the inverter in split-phase drives by means of a dual three-phase space vector classification algorithm," IEEE Trans. Ind. Electron., vol. 56, no. 1, pp. 120–129, Jan. 2009

[10] F. Barrero, J. Prieto, E. Levi, R. Gregor, S. Toral, M.J. Duran, M. Jones, "An Enhanced Predictive Current Control Method for Asymmetrical Six-Phase Motor Drives", IEEE Trans. Ind. Electron., vol.58, no.8, pp.3242,3252, Aug. 2011

[11] J. Karttunen, S. Kallio, P. Peltoniemi, P. Silventoinen, O. Pyrhonen, "Decoupled Vector Control Scheme for Dual Three-Phase Permanent Magnet Synchronous Machines," IEEE Trans. Ind. Electron., vol.61, no.5, pp.2185,2196, May 2014

[12] J. Hobraiche, J.P. Vilain, P. Macret, N. Patin, "A New PWM Strategy to Reduce the Inverter Input Current Ripples," IEEE Trans. Power Electr., vol.24, no.1, pp.172,180, Jan. 2009.

[13] The Dung Nguyen, N. Patin, G. Friedrich, "Extended Double Carrier PWM Strategy Dedicated to RMS Current Reduction in DC Link Capacitors of Three-Phase Inverters," IEEE Trans. Power Electron., vol.29, no.1, pp.396,406, Jan. 2014.

[14] W. Huiqing, X. Weidong,W. Xuhui, P.Armstrong, "Analysis and Evaluation of DC-Link Capacitors for High-Power-Density Electric Vehicle Drive Systems," IEEE Trans. on Vehicular Technology, vol.61, no.7, pp.2950,2964, Sept. 2012.

[15] L. Wook-Jin,S. Seung-Ki, "DC-Link Voltage Stabilization for Reduced DC-Link Capacitor Inverter," IEEE Trans. Ind. Appl., vol.50, no.1, pp.404,414, Jan-Feb. 2014.

[16] F. Locment, A. Bruyere, E. Semail, X. Kestelyn, J. M. Dubus, "Comparison of 3-, 5- and 7-leg Voltage Source Inverters for low voltage applications", Proc of IEMDC, May 2007, Turkey.

[17] R. Bojoi, M.C. Caponet, G. Grieco, M. Lazzari, A. Tenconi, F. Profumo, "Computation and measurements of the DC link current in six-phase voltage source PWM inverters for AC motor drives," Proc. of the Power Conversion Conference, 2002. PCC-Osaka 2002, vol.3, pp.953-958.

[18] A. Bouscayrol, X. Guillaud, P. Delarue, B. Lemaire-Semail, "Energetic Macroscopic Representation and inversion-based control illustrated on a wind energy conversion systems using Hardware-in-the-loop simulation", IEEE Trans. Ind. Electron., vol. 56, no. 12, pp. 4826-4835, Dec. 2009.

[19] A. Boglietti, R. Bojoi, A. Cavagnino, and A. Tenconi, "Efficiency analysis of PWM inverter fed three-phase and dual three-phase high frequency induction machines for low/medium power applications, " IEEE Trans. Ind. Electron., vol. 55, no. 5, pp. 2015–2023, May 2008.

[20] A. M. Hava, R. J. Kerkman, and T. A. Lipo, "Simple analytical and Graphical Methods for Carrier-Based PWM-VSI " IEEE Trans. Power Electron., vol. 14, no. 1, pp. 49–61, Jan. 1999

[21] A. Bouscayrol, B. Davat, B. de Fornel, B. François, J. P. Hautier, F. Meibody-Tabar, M. Pietrzak-David, "Multimachine Multiconverter System: application for electromechanical drives", European Physics Journal - Applied Physics, vol. 10, no. 2, pp. 131-147, May 2000

[22] Ph. Delarue, A. Bouscayrol, A. Tounzi, X. Guillaud, G. Lancigu, "Modelling, control and simulation of an overall wind energy conversion system", Renewable Energy, vol. 28, no. 8, pp. 1159-1324, July 2003